JOURNAL OF Materials CHEMISTRY Communication

Fabrication and characterization of highly-ordered periodic macroporous barium titanate by the sol–gel method

Zhibin Lei,[a] **Jianmin Li,***[a] **Yugen Zhang**[b] **and Sheming Lu**[a]

[a]*Department of Chemical Physics, University of Science and Technology of China, Hefei, Anhui, 230026, P.R. China. E-mail: jmli@ustc.edu.cn*
[b]*Department of Chemistry, University of Science and Technology of China, Hefei, Anhui, 230026, P.R. China*

Received 10th July 2000, Accepted 22nd September 2000
First published as an Advance Article on the web 1st November 2000

Highly-ordered three-dimensionally macroporous $BaTiO_3$ is prepared by template-directed synthesis and is structurally characterized.

In recent years the fabrication and characterization of three-dimensionally (3D) ordered macroporous materials have become one of the most hot and exciting areas. The main thrust of these intensive investigations stems from their wide range of applications: as membranes for separation and purification,[1] as high surface area adsorbents,[2] as solid support for sensors and catalysts,[3] as scaffolds for tissue engineering[4] and as photonic band gap materials for use in optoelectronics.[5] Colloidal arrays, owing to their 3D long-range order, have been widely used as good template candidates for the fabricatation of various porous materials ranging from inorganic oxides,[6–11] phosphates,[10] hybrid organosilicates,[10] diamond and glassy carbons[12] to various metals,[13,14] polymers[15–18] and chalcogenides.[19] Compared to bulk materials, these porous structure have many additional properties.

$BaTiO_3$ is one of the especially useful materials in the microelectronics industry. Because of its high dielectric constant, $BaTiO_3$ can be used as substrate and insulating layers in solid state displays[20] and flat panel displays based on electroluminescent and photochromic effects,[21] and as ultra-large scale integrated devices such as dynamic random access materials.[22,23] As a result, a great deal of work has been focused on the preparation of fine-grained $BaTiO_3$ powders. However, in this communication, we report the fabrication of 3D ordered macroporous $BaTiO_3$ by template-directed synthesis. In addition, the influence of the calcining temperature on the stability of the pores and on the crystallization of the solids has also been investigated. This novel 3D framework is expected to result in some new applications for $BaTiO_3$ such as photonic crystal separation and uses in optical devices.

In our work, we used a colloidal array of polystyrene (PS) spheres as the template. Nearly monodisperse PS spheres with an average diameter of 726 nm and relative standard deviation smaller than 4% (on the diameter) were obtained by emulsifier-free emulsion polymerization.[24] Before self-assembly, the PS spheres were washed with dilute aqueous ethanol by repeating the cycles of centrifugation and ultrasonic dispersion to eliminate unreacted starting materials and other impurities. A 3D ordered planar colloidal array of PS spheres was assembled by a modification of the method previously reported.[25] Impurity-free PS spheres were dispersed in aqueous ethanol (1 : 1 v/v) in a culture dish. After 5–7 days of self-assembly,[26–29] the suspending liquid was evaporated from the capillary, while the PS spheres spontaneously organized into an iridescent colloidal array, indicating that the arrangement of PS spheres is highly ordered. Fig. 1 shows a flowchart of the macroporous $BaTiO_3$ fabrication procedure. Firstly, 1 mmol $Ba(OH)_2$ was dissolved in 15 ml glacial acetic acid with stirring and heating, followed by condensation to 5 ml to get $Ba(AC)_2$ solution. Meanwhile, in an N_2 atmosphere 1 mmol titanium butoxide was diluted in absolute ethanol with a volume ratio of $Ti(C_4H_9O)_4 : C_2H_5OH = 1 : 2$. The precursor to $BaTiO_3$ was then prepared by adding $Ti(C_4H_9O)_4$ solution into the $Ba(AC)_2$ solution drop by drop under vigorous stirring. The concentration and viscosity of the precursor were adjusted by the amount of glacial acetic acid used in the preparation of $Ba(AC)_2$ solution. By capillary force, the precursor penetrated the voids between the dried PS spheres. We repeated the penetration and gelation many times (depending on the concentration of the precursor) in order to ensure that the voids were sufficiently filled. Lastly, solidifying the composite in a vacuum desiccator for 24 h and subsequently calcining the sample at 700 °C resulted in the formation of 3D macroporous $BaTiO_3$. A Hitachi X-650 scanning electron micrograph with an accelerating voltage of 25 KV was used to examine the morphology of the sample. A TG-DTA experiment was performed on a Shimadzu 50 H analyzer with a heating rate of $10\,^{\circ}C\ min^{-1}$ in the N_2 atmosphere. The powder X-ray diffraction patterns were determined at a scanning rate of $0.06^{\circ}\ s^{-1}$ in 2θ ranging from 10° to 70°, using a Y-4Q X-ray diffractometer with graphite monochromatized Cu Kα radiation ($\lambda = 1.54178$ Å).

During the self-assembly of the PS colloidal array, we found that the particle size distribution and the evaporating rate of the suspending solution of PS spheres have a significant effect on the template order. The broader the size distribution of PS spheres used, the more grain boundaries in the plane parallel to the substrate were found. Similar results were observed by Jiang[25] and Nagayama *et al.*[30] using silica spheres with relative standard deviations of 8% and 10% respectively. In addition, a fast solvent evaporation rate will also result in poor template. Besides many cracks on the surface, SEM shows that the colloidal crystal itself lacks long-range order. This is not surprising because rapid solvent evaporation relatively decreases the time for the PS spheres to find their location in the colloidal array. A poor template will result in a poor porous structure since the quality of any materials formed *via* template-directed syntheses depends mainly on the order and properties of the starting template.

Fig. 2 shows the scanning electron micrograph (SEM) images of the resulting macroporous $BaTiO_3$ made using a colloidal array of 726 nm spheres as template. Although the SEM images show that air spheres in $BaTiO_3$ have lattice parameters that are about 50% smaller than those of the starting PS spheres, the array of air spheres clearly have

DOI: 10.1039/b005555g

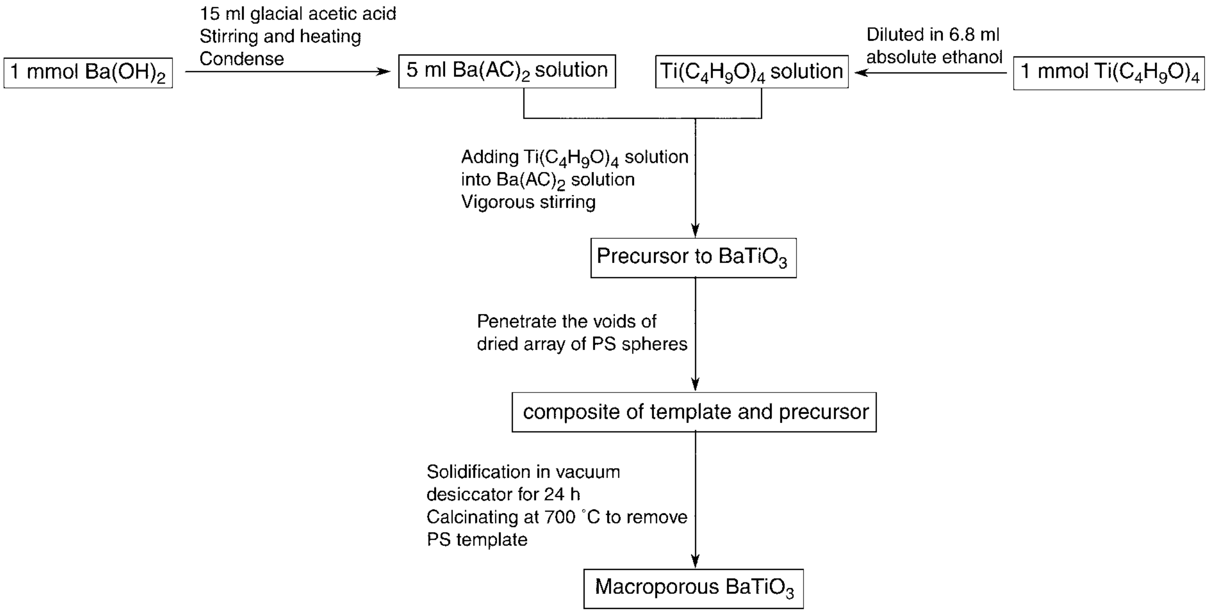

Fig. 1 Flowchart of the fabrication procedure of macroporous $BaTiO_3$.

retained the long-range order of the template and exhibits an ordered hexagonal close packing structure, see Fig. 2a. The next lower layer of pores is visible in Fig. 2b and the void spaces are interconnected in three dimensions through windows which form around the points where the starting PS spheres initially touched. Such a morphology has also been observed for many other porous materials using colloidal crystals as templates. In addition, like other inorganic macroporous materials, we can also see vacancies in Fig. 2b. The incomplete filling of voids between PS spheres and shrinkage during calcination are possibly responsible for this phenomenon.

As far as the removal of template is concerned, there are two approaches: extraction by solvent and calcination. Calcining is commonly used in the preparation of porous materials because, besides removal of the template, it can also permit the existence of a high-temperature solid phase reaction. In our work, we follow the latter to remove the PS sphere template. In fact, elemental analyses of the compound (Ti, 19.45%; Ba, 54.93%; C, 0.8%) also show only trace amounts of carbon, indicating that the treatment can remove almost all of the PS spheres. TG-DTA experiments are performed at the same time when calcining the sample. From the thermal analysis results we can see there are three zones of weight loss during calcination, see Fig. 3. The first one is obviously due to the vaporization of ethanol and decomposition of acetic acid and therefore corresponds to a wide endothermic phenomenon in the DTA data. The decomposition of organic ligands bound to the titanium and the combustion and gasification of PS spheres, between 260 °C and 420 °C of the second domain, lead to two exothermic peaks and simultaneously the formation of amorphous $BaCO_3$ and TiO_2[31] (see Fig. 3). The formation of macroporous $BaTiO_3$ undergoes the following solid phase reaction:[32]

$$BaCO_3 + TiO_2 \rightarrow BaTiO_3 + CO_2$$

The release of CO_2 results in the weight loss in the third zone at about 640 °C, from which $BaTiO_3$ starts to crystallize to hexagonal phase ($a_o = 5.735$, $c_o = 14.05$ Å), see Fig. 4b. The peak locations remain constant but their intensities increase with the calcining temperature increasing to 700 °C, and then the intensities decrease with the higher calcining temperature, see Fig. 4. In addition, we also investigated the dependence of the stability of the pore structure on the calcination

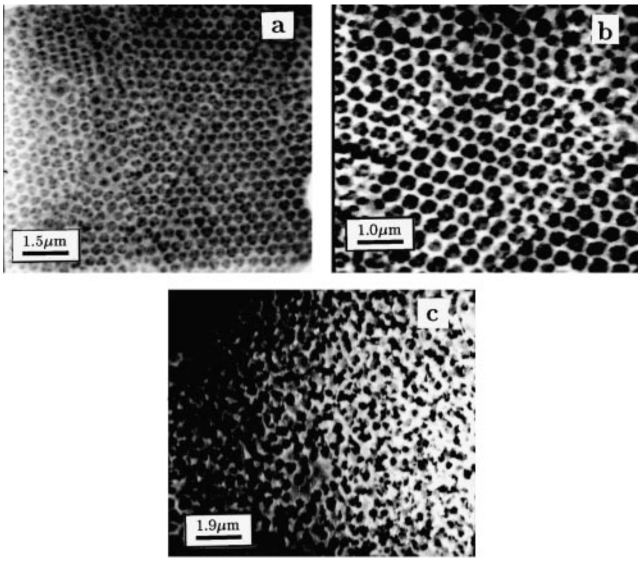

Fig. 2 Scanning electron micrograph images of typical macroporous $BaTiO_3$ formed using a colloidal array of 726 nm PS spheres as template: (a) $BaTiO_3$ after calcination at 700 °C for 6 hours has retained the initial long-range order of the PS spheres colloidal crystal and exhibits a close packed array; (b) details of air-sphere crystal of $BaTiO_3$ with the interconnected inner layer structure visible through the pores; (c) $BaTiO_3$ after calcination at 800 °C for 5 hours has lost the close packing structure.

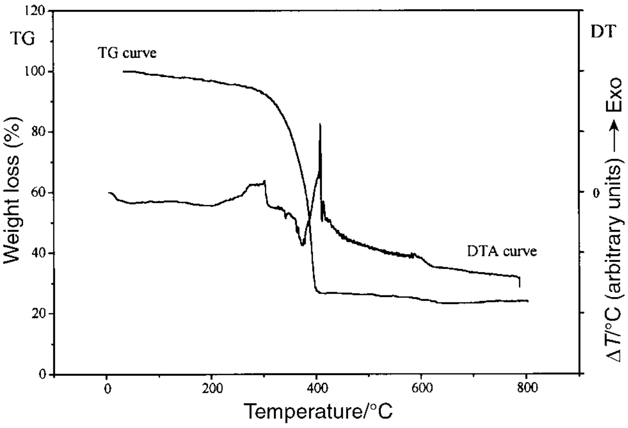

Fig. 3 TG-DTA curves during the calcination.

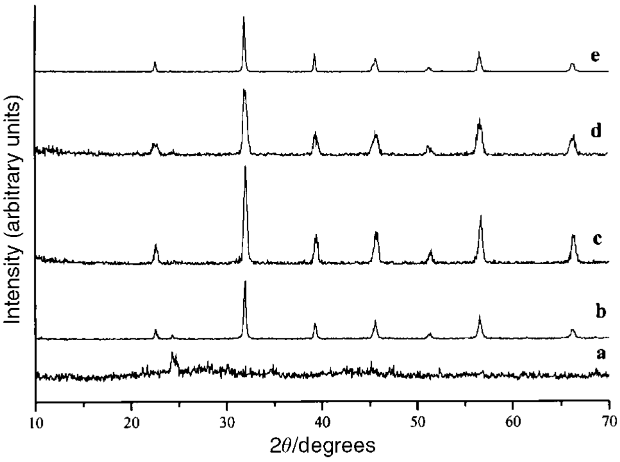

Fig. 4 Powder X-ray diffraction patterns of $BaTiO_3$ at different calcination temperatures: (a) 500 °C; (b) 640 °C; (c) 700 °C; (d) 750 °C; (e) 800 °C.

temperature. It is found that the porous structure can withstand temperatures ranging from 640 °C, the crystallization temperature, to at least 750 °C for 6 hours. Fig. 2c is the typical SEM image of a sample calcined at 800 °C for 5 hours. This image show that although the main scaffold is preserved, the array of ordered close packing of air spheres has been lost and a large number of the pores have deformed and collapsed.

In summary, macroporous $BaTiO_3$ with long-range order and a three-dimensionally periodic structure has been fabricated using a colloidal array of PS spheres as template. The air spheres of the resulting $BaTiO_3$ can be adjusted to the desired void volume by changing the particle size of the PS spheres of the initial template. Owing to its high dielectric constant, macroporous $BaTiO_3$ is expected to find many dielectric and optoelectric applications, as well as applications in fields such as separation and catalysis. Further investigations into the chemical and physical properties of macroporous $BaTiO_3$ are in progress.

Acknowledgements

We thank Professor Li Fanqing and Cheng Hao in the structure research laboratory of the University of Science and Technology of China for SEM measurements and we also thank National Natural Science Funds and National Education Ministry of China for financial support (No. 29871027).

Notes and references

1 R. R. Bhave, *Inorganic Membranes: Synthesis, Characteristics and Applications*, Van Nostrand Reinhold, New York, 1991.
2 D. E. Fain, *MRS Bull.*, 1994, **19**(4), 40.
3 V. S. Y. Lin, K. Motesharei, K. P. S. Dancil, M. J. Sailor and M. R. Chadin, *Science*, 1997, **278**, 840.
4 J. A. Hubbell and R. Langer, *Chem. Eng. News*, 1995 (March 13), 42.
5 J. D. Joannopoulos, P. R. Villeneuve and S. Fan, *Nature*, 1997, **386**, 143.
6 B. T. Holland, L. Abrams and A. Stein, *J. Am. Chem. Soc.*, 1999, **121**, 4308.
7 K. Qi, Z. Yang, Z. Liu, L. Wang and D. Zhao, *Sci. Bull. Sin.*, 2000, **45**, 267.
8 O. D. Velev, T. A. Jede, R. F. Lobo and A. M. Lenhoff, *Nature*, 1997, **389**, 447.
9 B. T. Holland, C. F. Blanford and A. Stein, *Science*, 1998, **281**, 538.
10 B. T. Holland, C. F. Blanford, T. Do and A. Stein, *Chem. Mater.*, 1999, **11**, 795.
11 J. E. G. J. Wijnhoven and W. L. Vos, *Science*, 1998, **281**, 802.
12 A. A. Zakhidov, R. H. Baughman, Z. Iqbal, C. Cui, I. Khayrullin, S. O. Dantas, J. Marti and V. G. Ralchenko, *Science*, 1998, **282**, 897.
13 O. D. Velev, P. M. Tessier, A. M. Lenhoff and E. W. Kaler, *Nature*, 1999, **401**, 548.
14 P. Jiang, J. Cizeron, J. F. Bertone and V. L. Colvin, *J. Am. Chem. Soc.*, 1999, **121**, 7957.
15 S. H. Park and Y. Xia, *Chem. Mater.*, 1998, **10**, 1745.
16 B. Gates, Y. Yin and Y. Xia, *Chem. Mater.*, 1999, **11**, 2827.
17 S. H. Park and Y. Xia, *Adv. Mater.*, 1998, **10**, 1045.
18 P. Jiang, K. S. Hwang, D. M. Mittleman, J. F. Bertone and V. L. Colvin, *J. Am. Chem. Soc.*, 1999, **121**, 11630.
19 P. V. Braun and P. Wiltzius, *Nature*, 1999, **402**, 603.
20 P. M. Alt, *Proc. SID*, 1984, **25**, 123.
21 X. Yang, A. H. Kitai and T. Xiao, *J. Appl. Phys.*, 1996, **79**, 3299.
22 M. H. Yeh, Y. C. Liu, I. N. Ln and J. Y. M. Lee, *J. Appl. Phys.*, 1993, **74**, 2143.
23 I. A. Burhanuddin, M. S. Tomar and E. Dayalan, *Thin Solid Films*, 1994, **253**, 53.
24 S. Zhu, J. Tu, X. Jin and L. Chen, *Acta Polym. Sin.*, 1998, **1**, 118.
25 P. Jiang, J. F. Bertone, K. S. Hwang and V. L. Colvin, *Chem. Mater.*, 1999, **11**, 2132.
26 N. D. Denkov, H. Yoshimura and K. Nagayama, *Ultramicroscopy*, 1996, 147.
27 A. S. Dimitrov and K. Nagayama, *Chem. Phys. Lett.*, 1995, **243**, 462.
28 M. Yamaki, J. Higo and K. Nagayama, *Langmuir*, 1995, **11**, 2975.
29 N. D. Denkov, O. D. Velev, P. A. Kralchevsky, I. B. Ivanov, H. Yoshimura and K. Nagayama, *Nature*, 1993, **361**, 26.
30 A. S. Dimitrov and K. Nagayama, *Langmuir*, 1996, **12**, 1303.
31 L. Christine, G. Bernard, M. Bernard, P. Jean-Paul and J. L. Andre, *J. Non-Cryst. Solids*, 1994, **175**, 1.
32 A. Mosset, I. Gautier-Luneau and J. Galy, *J. Non-Cryst. Solids*, 1988, **100**, 339.